Journal of Sound and Vibration (2002) **251**(4), 750–760
doi:10.1006/jsvi.2001.3843, available online at http://www.idealibrary.com on IDEAL®

THE LINEAR VIBRATION ANALYSIS OF MARINE RISERS USING THE WKB-BASED DYNAMIC STIFFNESS METHOD

Y. Cheng and J. Kim Vandiver

Department of Ocean Engineering, Massachusetts Institute of Technology, Cambridge, MA 02139-4307, *U.S.A.*

AND

G. Moe

Department of Structural Engineering, NTNU, Trondheim, Norway

(*Received* 19 *May* 2000, *and in final form* 5 *July* 2001)

1. INTRODUCTION

Marine risers are widely used in the offshore industry for a variety of purposes, such as deep water drilling, export and production. Slender marine risers are often subject to vortex-induced vibration (VIV), and therefore require accurate dynamic modelling for prediction of natural frequencies, mode shapes and fatigue damage rate. A typical marine riser tends to have a large characteristic length with rigid lumps and varying tension, flexural rigidity and mass density. The dynamic behavior of such a riser with variable properties and discontinuities is difficult to predict.

The VIV of marine risers has been studied extensively in recent years. Shear7, a program developed by Professor J. Kim Vandiver and his research group at MIT [1], uses modal analysis of uniform string and beam models with linearly varying tension to predict the cross-flow VIV response in steady, uniform or shear flows. Kim and Triantafyllou [2], assuming that the coefficients in the governing differential equation are continuous and slowly varying, used the WKB method to analyze a slender beam and derived some asymptotic solutions, which are implemented in Shear7. Recently, Moe *et al.* [3] have evaluated a variety of finite element approaches for the computation of natural frequencies of marine risers.

A great deal of theoretical research has focused on vibration analysis of tensioned beams. For a uniform Euler beam under a constant axial load, the effect of the axial load on the natural frequencies has been found by considering the natural frequencies to be functions of a non-dimensional load parameter and boundary conditions [4]. Using the dynamic stiffness method, Howson and Williams [5] discussed the natural frequencies of Timoshenko members under constant tension. For a uniform beam under a linearly varying axial load, Laird and Fauconneau [6] discussed the upper and lower bounds of natural frequencies. Using a power series expansion, Dareing and Huang [7] found natural frequencies of a uniform marine drilling riser.

A dynamic riser model is needed which is able to account for non-uniform properties such as mass density, bending rigidity and tension distribution, and discontinuities such as

0022-460X/02/140750 + 11 $35.00/0

intermediate supports. A closed-form solution to such a system is not generally possible. An approximation to the vibration analysis of such a riser may be accomplished by replacing the variable parameters with constant ones. For example, a variable axial load is often approximated by a tension that is constant over each element. However, many degrees of freedom in the approximation are required in order to obtain accurate results.

This paper investigates the vibration analysis of marine risers by combining the dynamic stiffness method [8–11] with the WKB theory [12, 13], which assumes that the coefficients in the differential equation of motion are slowly varying. The WKB-based dynamic stiffness matrix is first derived and the frequency-dependent shape function is expressed implicitly. Next the natural frequencies are found by equating to zero the determinant of the global dynamic stiffness matrix, which is obtained by following the procedure of the conventional finite element method. Finally, two examples of non-uniform risers are analyzed, and the results are compared to show the efficiency of this method.

2. DERIVATION OF THE WKB-BASED DYNAMIC STIFFNESS MATRIX

A general marine riser is a long slender beam system with variable tension distribution, bending rigidity and mass density. The mass/length changes are often discontinuous. Such a riser can be discretized into elements having continuously varying properties within the elements and allowing discontinuities to occur between elements. For each element, the WKB-based dynamic element stiffness matrix is derived by combining the dynamic direct-stiffness method [9] with the WKB approximation method [12, 13], which is a powerful tool for obtaining a global approximation to the solution of a linear differential equation.

The non-dimensional governing equation of motion of a riser can be written as [2]

$$\frac{\partial^2}{\partial s^2}\left[P(s)\frac{\partial^2 Y}{\partial s^2}\right]-\frac{\partial}{\partial s}\left[Q(s)\frac{\partial Y}{\partial s}\right]+U(s)\frac{\partial^2 Y}{\partial \tau^2}=f(s,\tau), \tag{1}$$

where

$$s=x/l,\qquad \tau=\omega_0 t,\qquad \omega_0=\sqrt{\frac{E_0I_0}{M_0l^4}},\qquad Y=\frac{w}{D_e},$$

$$P(s)=\frac{EI(ls)}{E_0I_0},\qquad Q(s)=\frac{T(ls)l^2}{E_0I_0},\qquad U(s)=\frac{m(ls)}{M_0}.$$

The subscript 0 represents the values at a reference cross-section, and the term $f(s,\tau)$ denotes a non-dimensional external force.

Letting $Y(s,\tau)=R(s)H(\tau)$, the equation for $R(s)$ is

$$\frac{\mathrm{d}^2}{\mathrm{d}s^2}\left[P(s)\frac{\mathrm{d}^2 R}{\mathrm{d}s^2}\right]-\frac{\mathrm{d}}{\mathrm{d}s}\left[Q(s)\frac{\mathrm{d}R}{\mathrm{d}s}\right]-U(s)\Lambda^2R=0. \tag{2}$$

Assuming that $P(s)$, $Q(s)$ and $U(s)$ in equation (2) vary slowly with respect to s, compared with variations of $R(s)$, $R'(s)$ and $R''(s)$, rewrite equation (2) as

$$\varepsilon^4P(z)\frac{\mathrm{d}^4R}{\mathrm{d}z^4}+2\varepsilon^4P'(z)\frac{\mathrm{d}^3R}{\mathrm{d}z^3}+[\varepsilon^4P''(z)-\varepsilon^2Q(z)]\frac{\mathrm{d}^2R}{\mathrm{d}z^2}-\varepsilon^2Q'(z)\frac{\mathrm{d}R}{\mathrm{d}z}-U(z)\Lambda^2R=0, \tag{3}$$

where $z\equiv\varepsilon s$, ε is a small parameter.

The formal WKB expansion is written as

$$R(z) \sim \exp\left[\frac{1}{\delta}\sum_{n=0}^{\infty}\delta^n S_n(z)\right], \quad \delta \to 0. \tag{4}$$

Substituting this equation into equation (3), identifying the same order terms, truncating the series and selecting $\delta = \varepsilon$, Kim and Triantafyllou [2] found the asymptotic solution by taking first two terms in equation (4),

$$R(s) = T_2(s)\left[C_1 \sin\left(\int_0^s h_2(\xi)\,\mathrm{d}\xi\right) + C_2 \cos\left(\int_0^s h_2(\xi)\,\mathrm{d}\xi\right)\right] + T_1(s)\left[C_3 \sinh\left(\int_0^s h_1(\xi)\,\mathrm{d}\xi\right) + C_4 \cosh\left(\int_0^s h_1(\xi)\,\mathrm{d}\xi\right)\right], \tag{5}$$

where

$$T_1(s) = \frac{1}{\sqrt{P}}\left[\frac{1}{2}\left(\frac{Q}{P}\right)^3 + 2\frac{QU\Lambda^2}{P^2} + \frac{1}{2}\left(\left(\frac{Q}{P}\right)^2 + 4\frac{U\Lambda^2}{P}\right)^{3/2}\right]^{-1/4},$$

$$T_2(s) = \frac{1}{\sqrt{P}}\left[-\frac{1}{2}\left(\frac{Q}{P}\right)^3 - 2\frac{QU\Lambda^2}{P^2} + \frac{1}{2}\left(\left(\frac{Q}{P}\right)^2 + 4\frac{U\Lambda^2}{P}\right)^{3/2}\right]^{-1/4},$$

$$h_1(s) = \sqrt{\frac{1}{2}\frac{Q}{P} + \frac{1}{2}\sqrt{\left(\frac{Q}{P}\right)^2 + 4\frac{U\Lambda^2}{P}}}, \qquad h_2(s) = \sqrt{-\frac{1}{2}\frac{Q}{P} + \frac{1}{2}\sqrt{\left(\frac{Q}{P}\right)^2 + 4\frac{U\Lambda^2}{P}}}.$$

Note that:

$$\frac{\mathrm{d}w}{\mathrm{d}x} = \frac{D_e}{l}\frac{\mathrm{d}Y}{\mathrm{d}s}, \quad \frac{\mathrm{d}^2 w}{\mathrm{d}x^2} = \frac{D_e}{l^2}\frac{\mathrm{d}^2 Y}{\mathrm{d}s^2}, \quad \frac{\mathrm{d}^3 w}{\mathrm{d}x^3} = \frac{D_e}{l^3}\frac{\mathrm{d}^3 Y}{\mathrm{d}s^3}.$$

Taking a first order approximation, then the nodal displacement vector $\mathbf{V}_F$, can be formulated in matrix form as

$$\begin{pmatrix} v_{1y} \\ \theta_1 \\ v_{2y} \\ \theta_2 \end{pmatrix} = D_e \begin{bmatrix} 0 & T_2(0) & 0 & T_1(0) \\ \dfrac{T_2(0)h_2(0)}{l} & 0 & \dfrac{T_1(0)h_1(0)}{l} & 0 \\ B_1 T_2(1) & B_2 T_2(1) & B_3 T_1(1) & B_4 T_1(1) \\ \dfrac{B_2 T_2(1) h_2(1)}{l} & -\dfrac{B_1 T_2(1) h_2(1)}{l} & \dfrac{B_4 T_1(1) h_1(1)}{l} & \dfrac{B_3 T_1(1) h_1(1)}{l} \end{bmatrix} \begin{pmatrix} C_1 \\ C_2 \\ C_3 \\ C_4 \end{pmatrix}. \tag{6}$$

Equation (6) can be written in abbreviated form as

$$\mathbf{V}_F = D_e \mathbf{G}\mathbf{C}. \tag{7}$$

The nodal forces, $\mathbf{F}$, for an element with changing properties can be written as

$$m_1 = -EI(x)D_e \left.\frac{\mathrm{d}^2 R}{\mathrm{d}x^2}\right|_{x=0} = -\frac{EI(s)D_e}{l^2}\left.\frac{\mathrm{d}^2 R}{\mathrm{d}s^2}\right|_{s=0} = -P(s)\frac{E_0 I_0 D_e}{l^2}\left.\frac{\mathrm{d}^2 R}{\mathrm{d}s^2}\right|_{s=0}, \tag{8}$$

$$m_2 = EI(x)D_e \frac{d^2R}{dx^2}\bigg|_{x=l} = \frac{EI(s)D_e}{l^2}\frac{d^2R}{ds^2}\bigg|_{s=1} = P(s)\frac{E_0 I_0 D_e}{l^2}\frac{d^2R}{ds^2}\bigg|_{s=1}, \tag{9}$$

$$s_{1y} = -EI(x)D_e\frac{d^3R}{dx^3}\bigg|_{x=0} - T(x)D_e\frac{dR}{dx}\bigg|_{x=0} = \frac{EI(s)D_e}{l^3}\frac{d^3R}{ds^3}\bigg|_{s=0} - \frac{T(s)D_e}{l}\frac{dR}{ds}\bigg|_{s=0}, \tag{10}$$

$$s_{2y} = -\left(EI(x)D_e\frac{d^3R}{dx^3}\bigg|_{x=l} - T(x)D_e\frac{dR}{dx}\bigg|_{x=l}\right) = -\frac{EI(s)D_e}{l^3}\frac{d^3R}{ds^3}\bigg|_{s=1} + \frac{T(s)D_e}{l}\frac{dR}{ds}\bigg|_{s=1}. \tag{11}$$

Substituting for $R(s)$ from equation (5), equations (8–11) can be written in the matrix form

$$\mathbf{F} = D_e\mathbf{DC}, \tag{12}$$

where the non-zero elements of the matrix $\mathbf{D}$ are

$$D(1,1) = -\frac{E_0 I_0}{l^3}(P(0)T_2(0)h_2^3(0) - Q(0)T_2(0)h_2(0)),$$

$$D(1,3) = \frac{E_0 I_0}{l^3}(P(0)T_1(0)h_1^3(0) - Q(0)T_1(0)h_1(0)),$$

$$D(2,2) = \frac{P(0)E_0 I_0}{l^2}T_2(0)h_2^2(0), \qquad D(2,4) = -\frac{P(0)E_0 I_0}{l^2}T_1(0)h_1^2(0),$$

$$D(3,1) = \frac{E_0 I_0}{l^3}(P(1)T_2(1) + Q(1)T_2(1)h_2(1)),$$

$$D(3,2) = -\frac{E_0 I_0}{l^3}(P(1)T_2(1)h_2^3(1) + Q(1)T_2(1)h_2(1)),$$

$$D(3,3) = -\frac{E_0 I_0}{l^3}(P(1)T_1(1)h_1^3(1) + Q(1)T_1(1)h_1(1)),$$

$$D(3,4) = -\frac{E_0 I_0 B_3}{l^3}(P(1)T_1(1)h_1^3(1) + Q(1)T_1(1)h_1(1)),$$

$$D(4,1) = -\frac{P(1)E_0 I_0}{l^2}B_1 T_2(1)h_2^2(1), \qquad D(4,2) = -\frac{P(1)E_0 I_0}{l^2}B_2 T_2(1)h_2^2(1),$$

$$D(4,3) = \frac{P(1)E_0 I_0}{l^2}B_3 T_1(1)h_1^2(1), \qquad D(4,4) = \frac{P(1)E_0 I_0}{l^2}B_4 T_1(1)h_1^2(1).$$

Combining equation (7) with equation (12) leads to

$$\mathbf{F} = \mathbf{K}\mathbf{V}_F, \tag{13}$$

where $\mathbf{K} = \mathbf{DG}^{-1}$ is the WKB-based dynamic element stiffness matrix, whose elements are derived by using Maple V [14].

3. FREQUENCY-DEPENDENT SHAPE FUNCTION

In order to derive the frequency-dependent shape function, rewrite equation (5) as

$$\mathbf{R}\,(s) = \begin{bmatrix} T_2(s)\sin\int_0^s h_2(\xi)\,\mathrm{d}\xi \\ T_2(s)\cos\int_0^s h_2(\xi)\,\mathrm{d}\xi \\ T_1(s)\sinh\int_0^s h_1(\xi)\,\mathrm{d}\xi \\ T_1(s)\cosh\int_0^s h_1(\xi)\,\mathrm{d}\xi \end{bmatrix}^{\mathrm{T}} \begin{pmatrix} C_1 \\ C_2 \\ C_3 \\ C_4 \end{pmatrix}. \tag{14}$$

Solving for **C** from equation (7) and substituting it into equation (14) results in

,

$$\mathbf{R}(s) = \Phi \mathbf{V}_F, \tag{15}$$

where Φ is the frequency-dependent shape function obtained by means of Maple V.

4. NATURAL FREQUENCIES AND MODE SHAPES

With the derived local WKB-based dynamic stiffness element matrix **K** in equation (13), one can obtain the global dynamic stiffness matrix by following the procedure of the conventional finite element method [15], in which local elements are cast into global form by co-ordinate transformations. Then, boundary conditions are imposed. Finally, the equation of motion of free vibration in the restrained global dynamic stiffness form can be written as

$$\mathbf{K}_G(\omega)\mathbf{X} = 0. \tag{16}$$

It is noted that the global dynamic stiffness matrix $\mathbf{K}_G$ is implicitly non-linear with respect to frequency. Solving its eigenvalues is not generally straightforward. Natural frequencies can be found by equating the determinant of $\mathbf{K}_G$ to zero. They are obtained by plotting the figure of $\det[\mathbf{K}_G(\omega)]$ versus ω.

Once the natural frequencies are found, one can use equation (16) to solve for a specific mode vector. An effective way is to use a triangular decomposition. For a specific natural frequency, ω_n, one can use the Gauss elimination to decompose $\mathbf{K}_G(\omega_n)$ as

$$\mathbf{K}_G(\omega_n) = [\mathbf{L}_n]\,[\mathbf{U}_n], \tag{17}$$

where $[\mathbf{L}_n]$ is a lower triangular matrix and $[\mathbf{U}_n]$ is an upper triangular matrix. Then the nth eigenvector is solved from

$$[\mathbf{U}_n]\mathbf{X}_n = 0, \tag{18}$$

where $\mathbf{X}_n \equiv [x_1, x_2, \ldots, x_n]^{\mathrm{T}}$ and

$$\mathbf{U}_n \equiv \begin{bmatrix} u_{1,1} & u_{1,2} & \cdots & \cdots & u_{1,n} \\ & u_{2,2} & \cdots & \cdots & u_{2,n} \\ & & \ddots & \vdots & \vdots \\ & & & u_{n-1,n-1} & u_{n-1,n} \\ & & & & u_{n,n} \end{bmatrix}.$$

Assume $x_n = 1$, the $(n-1)$th row in equation (18) gives

$$u_{n-1,n-1}x_{n-1} + u_{n-1,n} = 0, \tag{19}$$

then,

$$x_{n-1} = -\frac{u_{n-1,\,n}}{u_{n-1,\,n-1}}. \tag{20}$$

Similarly, from the $(n-2)$ row in equation (18) one can obtain

$$x_{n-2} = -\frac{u_{n-2,\,n-1}x_{n-1} + u_{n-2,n}}{u_{n-2,n-2}} \tag{21}$$

The general recurrence relation can be written as

$$x_i = -\frac{\sum_{k=i+1}^{n} u_{i,k}x_k}{u_{i,i}} \quad (i = 1, \ldots, n-1). \tag{22}$$

Hence, mode components at element nodes are calculated from the above formulas. Different from a conventional FEM, the displacements at nodes are not necessarily indicative of what is occurring within elements. Hence, post-processing is necessary to obtain mode shapes. One can use equation (15) to calculate mode components for any point within an element. In this way, accurate mode shapes can be obtained.

On the basis of the above procedure, Matlab codes for solving natural frequencies and mode shapes for marine risers were developed.

5. NUMERICAL EXAMPLES

5.1. AN EXAMPLE OF A UNIFORM DRILLING RISER UNDER LINEARLY VARYING TENSION [7]

The parameters of a simply supported riser are length $l = 152{\cdot}4$ m; outer diameter $d_o = 0{\cdot}6096$ m; thickness $t = 0{\cdot}0159$ m; Young's modulus $E = 2{\cdot}07 \times 10^{11}$ N/m^2; moment of inertia $I = 1{\cdot}30 \times 10^{-3}$ m^4; mass per unit length $m = 995{\cdot}92$ kg/m (includes mass of drilling mud and seawater); tension at the bottom ball joint $T_0 = 1{\cdot}27 \times 10^6$ N; net weight of riser per unit length in seawater $w = 3{\cdot}12 \times 10^3$ N/m (includes 554·79 N/m for choke and kill lines); cross-sectional area of the riser exterior $A_e = 0{\cdot}2917$ m^2; cross-sectional area of the riser interior $A_i = 0{\cdot}2278$ m^2; density of seawater $\rho_w = 1038{\cdot}9$ kg/m^3; density of drilling mud $\rho_m = 1362{\cdot}8$ kg/m^3.

This riser was discretized into five elements with equal length. Using the WKB-based dynamic stiffness method, Table 1 shows the first five natural frequencies. In order to verify

TABLE 1

Comparison of circular natural frequencies

Order	Dareing and Huang [7]	FEM (60 elements)	WKB-DSSM (5 elements)
1	0·8150	0·8150	0·8150
2	1·8036	1·8038	1·8037
3	3·0876	3·0879	3·0878
4	4·7375	4·7377	4·7377
5	6·7890	6·7896	6·7896

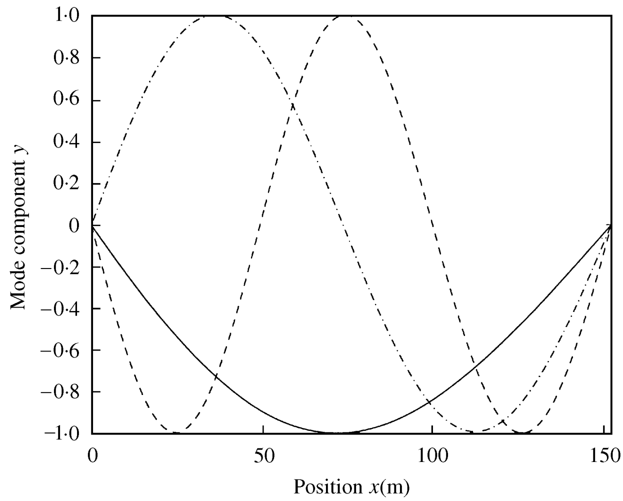

Figure 1. The first three natural mode shapes for a 500-ft riser: ———, first mode; – · – · – · – ·, second mode; -----, third mode.

the results, a finite element procedure which assumed constant tension over each beam element was developed. Converged values for natural frequencies were found employing 60 elements. The approximation result [7] previously obtained by means of a power series expansion is also included for comparison. It is observed from Table 1 that the natural frequencies acquired by the WKB-based dynamic stiffness method using only five elements are accurate to order $O(10^{-4})$. Measuring the position $x(m)$ from the bottom, Figure 1 depicts the first three mode shapes.

Table 1 depicts that the natural frequencies obtained by Dareing and Huang [7] are close to those found using the FEM and the WKB-based dynamic stiffness method. However, their finding of "points of inflection" in mode shapes is not correct.

5.2. AN EXAMPLE OF A NON-UNIFORM RISER WITH VARIABLE PROPERTIES

Due to attachments such as buoyancy modules, a typical marine riser is a system with variable properties including tension and mass density. The simply supported Helland–Hanson riser is one such riser, with the following specifications: length $L = 689{\cdot}29$ m; outer steel diameter $d_o = 0{\cdot}5334$ m; inner steel diameter $d_i = 0{\cdot}5016$ m; buoyancy diameter $d_b = 1{\cdot}1303$ m.

Figures 2 and 3 shows the variations of the mass density and tension at the measured points which are marked respectively. The position is measured from the bottom. These figures demonstrate that the mass density does not change continuously, and tension does not vary linearly.

Using the WKB-based dynamic stiffness method, the riser was discretized into 11 elements. Figure 4 shows the first 20 natural frequencies. The approximated results using Shear7 [1], which assumed the riser to be an equivalent uniform beam with linearly varying tension, are included for comparison. The Shear7 results are accurate for lower order natural frequencies.

Figure 5 depicts the 20th mode shape, which is of interest. The locations of the antinodes are not evenly spaced. Therefore, the mode differs from trigonometric ones.

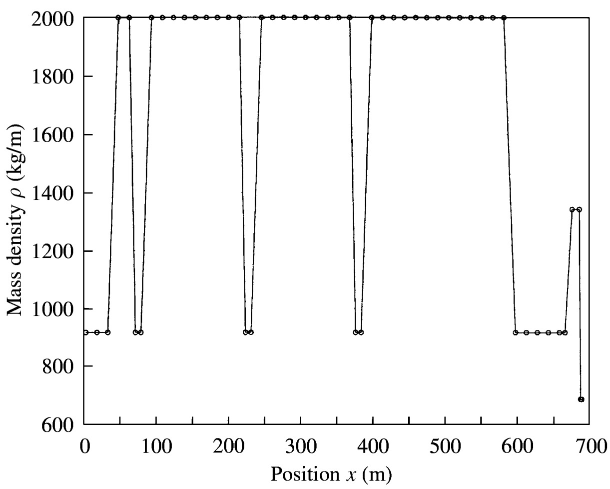

Figure 2. The mass density variation of the Helland riser.

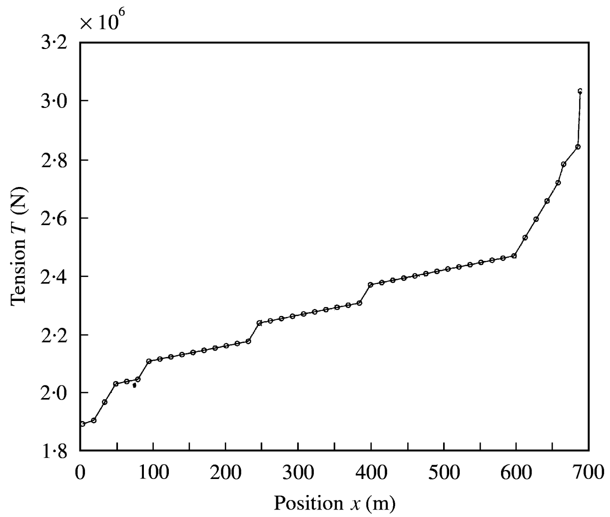

Figure 3. The tension variation of the Helland riser.

It is found that 282 elements are needed for the standard finite element method to obtain a good 20th mode shape and a converged natural frequency of 0·6952 Hz. This is close to 0·6955 Hz by the WKB-based dynamic stiffness method with only 11 elements. Very few elements are necessary if they are chosen wisely. Within each element, properties must vary slowly so as to satisfy the WKB assumptions. Discontinuities should occur at the junctions of elements. In this example, the mass/length changes abruptly 10 times requiring a total of 11 elements to adequately model the system.

6. CONCLUSIONS

Natural frequencies and mode shapes are important information for predicting the VIV of marine risers. The WKB-based dynamic stiffness method has been introduced to analyze

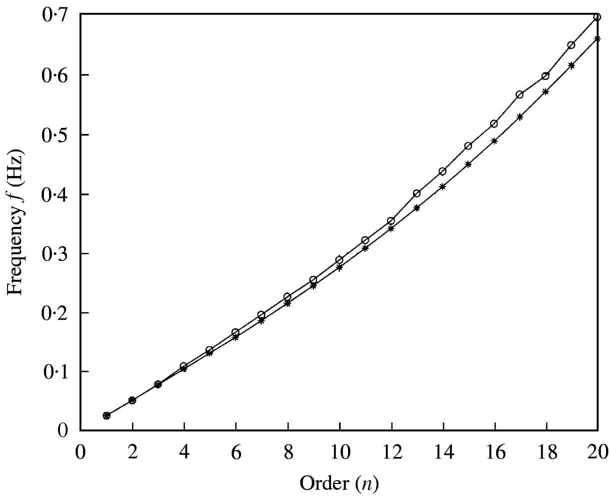

Figure 4. The comparison of the natural frequencies with those obtained by Shear7: ○, DSM; *, by Shear7.

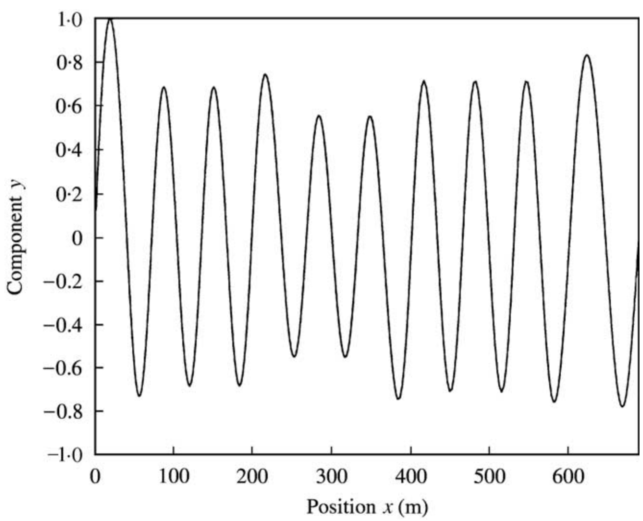

Figure 5. The 20th mode shape of the Helland riser (freq = 0·6955 Hz).

non-uniform marine risers on the assumption that the properties are slowly varying within elements. When compared with a conventional finite element method, the present method demonstrates some advantages, such as eliminating spatial discretization error since the accurate asymptotic solution is used within elements and finding accurate natural frequencies by means of a limited number of elements.

In the determination of natural frequencies from equation (16), it is noted that $\mathbf{X} = 0$ is not necessarily a trivial set of solutions but corresponds, sometimes, to a mode shape whose nodes are nodes of the FEM. For uniform members, it is possible to derive an infallible search algorithm [16], but it does not seem to be so easy for non-uniform beams under linearly varying tension. One way of overcoming this difficulty is to calculate and store all natural frequencies of clamped–clamped non-uniform members and then apply the Wittrick–William algorithm [5, 17].

ACKNOWLEDGMENTS

This project was sponsored by the Office of Naval Research and by a consortium of companies. The consortium included ARCO, BP/Amoco, Chevron, Exxon/Mobil, Norsk Hydro, Petrobras, Shell, Statoil, Texaco and CSO-Aker Engineering.

REFERENCES

1. J. K. VANDIVER 1998 *Notes From a Workshop On the Prediction of Vortex-Induced Vibration of Marine Risers Using Shear7 Program* **1**. Cambridge: Massachusetts Institute of Technology.
2. Y. C. KIM and M. S. TRIANTAFYLLOU 1984 *Journal of Energy Resources technology* **250**. The nonlinear dynamics of long slender cylinders.
3. G. MOE, Y. CHENG and J. K. VANDIVER 2000 *Proceedings of ETCE/OMAE2000 Joint Conference*. New Orleans, LA, U.S.A. Riser analysis by means of some finite element approaches.
4. R. D. BLEVINS 1984 *Formulas for Natural Frequency and Mode Shape*. Malabar, FL: Robert E. Krieger.
5. W. P. HOWSON and F. W. WILLIAMS 1995 *Journal of Sound and Vibration* **26**, 503–515. Natural frequencies of frames with axially loaded Timoshenko members.
6. W. M. LAIRD and G. F. AUCONEAU 1966 *National Aeronautics and Space Administration Report NASA-CR*-653. Upper and lower bounds for the eigenvalues of vibrating beams with linearly varying axial load.
7. D. W. DAREING and T. HUANG 1976 *Journal of Petroleum Technology*, 813–818. Natural frequencies of marine drilling risers.
8. A. Y. T. LEUNG and W. E. ZHOU 1995 *Journal of Sound and Vibration* **181**, 447–456. Dynamic stiffness analysis of non-uniform Timoshenko beams.
9. R. W. CLOUGH and J. PENZIEN 1975 *Dynamics of Structures*. New York: McGraw-Hill Book Company Inc.
10. T. H. RICHARDS and Y. T. LEUNG 1977 *Journal of Sound and Vibration* **55**, 363–376. An accurate method in structural vibration analysis.
11. F. VENANCIO-FILHO 1996 *Journal of Sound and Vibration* **198**, 639–640. Comments on: an exact model reduction technique for beam structures: combination of transfer and stiffness matrices.
12. C. M. BENDER and S. A. ORSZAG 1978 *Advanced Mathematical Methods for Scientists and Engineers*. New York: McGraw-Hill Book Company.
13. R. B. PARIS and A. D. WOOD 1986 *Asymptotics of High Order Differential Equation*. New York: John Wiley Sons Inc.
14. A. HECK 1996 *Introduction to Maple*. New York: Springer-Verlag; second edition.
15. K. J. BATHE 1996 *Finite Element Procedures*. New Jersey: Prentice-Hall International Inc.
16. P. SWANNELL 1973 *Theory and Practice in Finite Element Structural Analysis*. Tokyo: University of Tokyo Press. The automatic computation of the natural frequencies of structural frames using an exact matrix technique.
17. J. R. BANERJEE and F. W. WILLIAMS 1985 *Journal of Sound and Vibration* **21**, 2289–2302. Exact Bernoulli–Euler dynamic stiffness matrix for a range of tapered beams.

APPENDIX A: NOMENCLATURE

B_i	$B_i(1)$ c ($i = 1$–4)
$B_1(s)$	$\sin \int_0^s h_2(\xi)\,\mathrm{d}\xi$
$B_2(s)$	$\cos \int_0^s h_2(\xi)\,\mathrm{d}\xi$
$B_3(s)$	$\sinh \int_0^s h_1(\xi)\,\mathrm{d}\xi$
$B_4(s)$	$\cosh \int_0^s h_1(\xi)\,\mathrm{d}\xi$
C_i	constants of integration ($i = 1$–4)
D_e	effective diameter of riser
E	Young's modulus of beam material
$F(x, t)$	external force
$f(s, \tau)$	$F(s, \tau) l^4 / D_e E_0 I_0$

$I(x)$	area moment inertia of the beam
l	length of a riser element
$m(x)$	mass of the beam per unit length
M_0	reference mass per unit length
$P(s)$	dimensionless bending rigidity
$Q(s)$	dimensionless tension
$U(s)$	dimensionless mass density
s	dimensionless distance
$T(x)$	tension of the beam per unit length
w	transverse displacement of riser
x	vertical co-ordinate measured in axial direction of riser
Y	dimensionless deflection
ω_0	reference frequency
τ	dimensionless time
Λ	dimensionless frequency, ω/ω_0